Dynamical Transitions in a Coupled Integrated Device

B. Cemlyn, D. Labukhin. M. J. Adams and I. D. Henning
School of Computer Science and Electronic Engineering, University of Essex
Colchester, CO4 3SQ UK, brceml@essex.ac.uk

***Abstract* — We show how the degree of mutual and self-coupling within an integrated device can be determined using two different methods combining modelling and experiment. This coupling magnitude is then used to find the boundaries of nonlinear dynamics (NLD) in the device. The dependence of these boundaries on the coupling magnitude reflects a general trend and is an important reference for the design of photonic integrated circuits (PICs).**

I. INTRODUCTION

Characterising the dynamical regimes of PICs is essential for their development [1]. One of the common causes of NLD in semiconductor lasers is the interaction of its internal field and carriers with a perturbing optical field, created either by reflection or an external source. Due to high sensitivity of NLD to device parameters, even such small factors as parasitic reflection can play a significant role and must be taken into account.

Here we investigate NLD of an integrated device featuring two coupled lasers and the dependence of the dynamics transitions on the coupling strength and detuning between the two lasers. Since the coupling is caused by facet reflection, our study starts by calibrating the reflection using a combination of modelling and experiment. Then, its value is used in the modelling of laser dynamics to determine the ranges of coupling strength and detuning that produce NLD. Experimental data are presented to validate these results.

II. PIC UNDER STUDY

The PIC studied here is shown in Fig. 1. It consists of two twin DBR lasers, of lasing wavelengths 1561 and 1555 nm, coupled into an SOA [2]. The lasers' DBR sections enable the detuning between them to be altered from 0 to 1 THz (0-8 nm). Reflection from the front facet and an aligned fibre provides self- and cross-coupling between the lasers that can trigger NLD, depending on the SOA gain and the detuning between the lasers.

We characterise the coupling as the total power reflection R_{tot}, which is a function of the reflection at the cleaved facet, R_{cf}, and the SOA gain squared (to account for amplification in both directions) $R_{tot} = R_{cf} G_{SOA}^2 / 2$. We use a travelling wave model [3] that shows a full spatial-temporal dynamics of the field and carrier density, enabling us to derive R_{tot}. However, matching the model and experiment requires calibration as neither R_{cf} nor G_{SOA} is known with sufficient accuracy. The overall effect of R_{tot} can be seen in two phenomena: the transition to NLD and irregularity of the tuning behaviour. Comparing modelled and experimental data for varying values of G_{SOA} (controlled by the SOA current I_{SOA}) will allow us to find R_{cf} and then derive R_{tot}.

III. CALIBRATION OF MODEL

For calibration by the dynamical transition, the optical spectrum of the device was experimentally recorded with a range of SOA currents and detunings between the lasers. Fig. 2(a-c) show the change of the spectra as one laser is tuned in the vicinity of the other's wavelength, while the latter is kept constant. Broad dynamical spectra appear at different detunings and SOA currents; however, a transition to NLD across the tuning range is apparent at I_{SOA} = 20 mA.

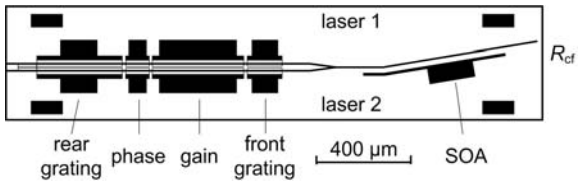

Fig. 1. Integrated chip with two twin DBR lasers and SOA.

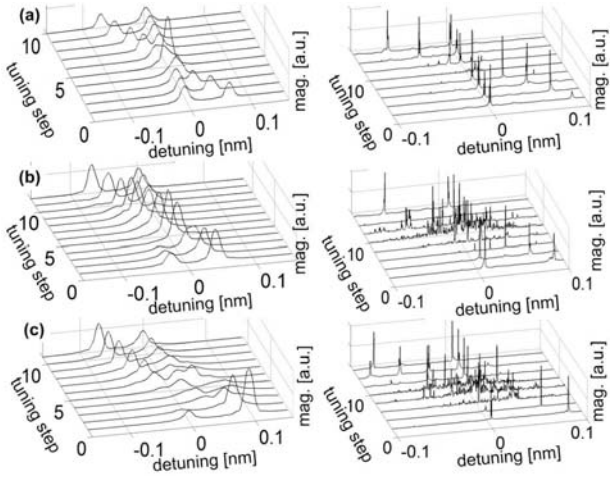

Fig. 2. Optical spectra for different values of I_{SOA}: (a) 5 mA, (b) 15 mA and (c) 20 mA; measured data is in the right column, modelled in the left. The coupling between the two lasers increases with I_{SOA}, and NLD, characterised by a broad flat spectrum, ensue.

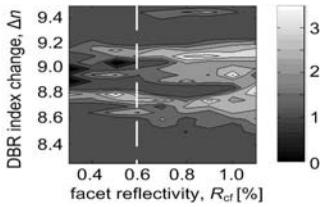

Fig. 3. Modelled dynamics map as the function of the DBR index detuning Δn (the tuned laser) and reflectivity R_{cf} for I_{SOA} = 20 mA. The dimension increasing above unity as the reflectivity increases. The dashed line shows the appearance of high-dimensional dynamics.

Next, in order to calibrate R_{cf}, the model was set up with I_{SOA} = 20 mA and a range of R_{cf}, and the dynamics types were quantified using a correlation dimension algorithm [4]. Before the transition to NLD, the only dynamics are mode-beating between the two lasing frequencies. These periodic dynamics have a dimension of one, whereas NLD have a dimension significantly greater than one. Therefore the transition point in terms of R_{cf} can be identified from an increase in the correlation dimension. Fig. 3 shows these results, from which R_{cf} was estimated as 0.6% and translates to an R_{tot} magnitude of 0.3%.

The second method of calibration involves the tuning behaviour of one of the lasers. Under zero reflection, the dependence of the lasing wavelength on the DBR index, n_{DBR}, is a staircase function, with periodic wavelength jumps (Fig. 4a). It was reported in [5] that, as R_{tot} increases, the tuning periods between the jumps begin to display increasing irregularity (Fig. 4b). This is due to the external cavity modes, that re-enforce or weaken the main lasing mode (depending on their phase), and thus change the condition under which it switches to the next main-cavity mode. The difference between the longest and the shortest periods increases with the absolute value of R_{tot}

The experimental tuning curves as functions of the DBR current I_{DBR} were obtained for five values of I_{SOA} from 5 to 25 mA. The relationship between I_{DBR} and the effective refractive index n_{DBR} is found from the mode-jumping points at I_{SOA} = 5 mA (corresponding to low R_{tot}), since these points are symmetrically positioned with respect to the Bragg wavelength $\lambda_{DBR} = 2\Lambda n_{DBR}$, where Λ is the grating period. Next, the experimental curves were plotted against n_{DBR} (Fig. 4) and the total dispersion of tuning periods as a function of I_{SOA} was obtained (Fig. 5). Finally, we simulate families of tuning curves for the same set of I_{SOA} values and several values of R_{cf}. We found that R_{cf} = 0.5% gives the best fitting for the experimental curve in Fig. 5. This is in a good agreement with the value obtained from analysing detuning ranges of NLD.

IV. Detuning Dependence of the Dynamical Transition

After the calibration of the model, the detuning-dependent dynamical transition can be further investigated. Fig. 2(a-c) show that for low values of I_{SOA} (where G_{SOA} is less or approximately equal to one), the dynamical transition occurs within a small range, which then grows with the increase of I_{SOA}. This dependence, extracted from the experimental and modelled data, is shown in Fig. 6. The two curves show a good agreement.

It is also interesting that as I_{SOA} increases the NLD shows more and more complex structure; thus, for I_{SOA}=25 mA, we can observe high-dimensional chaotic dynamics.

V. Conclusions

We have shown how the factors of coupling magnitude and detuning affect the dynamical transitions in a PIC consisting of two DBR lasers coupled through a facet reflection. It is critical in the development of PICs that these boundaries are well defined and understood.

A travelling-wave model and experimental data were used to characterize the reflection in the PIC and then to find

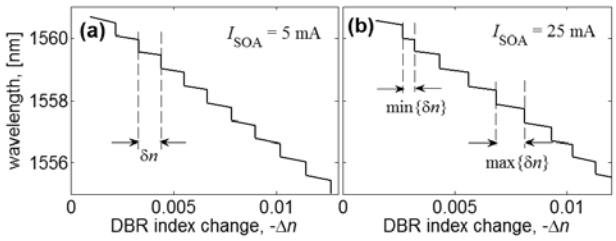

Fig. 4. Experiment: lasing wavelength vs. DBR index change (negative) for different SOA currents. I_{SOA} = 5 mA results in low R_{tot} and periodic tuning curve. I_{SOA} = 25 mA results in high R_{tot} and irregular tuning curve.

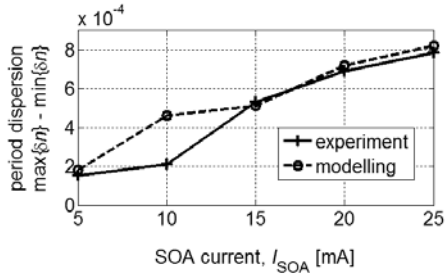

Fig. 5. Experiment and simulation. Tuning period dispersion vs. SOA current. Solid line: experiment; dashed line: modelling for R_{cf} = 0.5%.

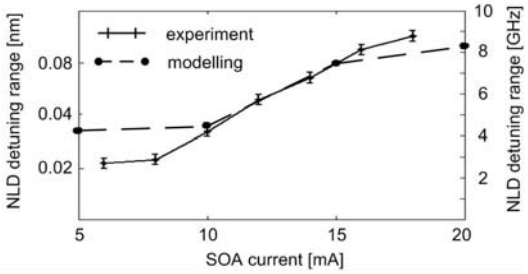

Fig. 6. The detuning ranges within which NLD is observed vs. SOA current for R_{cf} = 0.5%.

tuning boundaries of NLD. Simulated and experimental curves showed a good agreement, validating the model. It was shown that even relatively small reflection significantly affects the device's dynamics.

It also was demonstrated both experimentally and numerically that the detuning ranges of NLD, as well as the complexity of the dynamics, grows with the increase of the coupling strength between two lasers, controlled by the SOA current and the chip-to-fibre reflection. In particular, this dependence can be employed in applications requiring high-dimensional chaos.

References

[1] M. Yousefi, Y.Barbarin, S. Beri, E. A. J. M. Bente, M. K. Smit, R. Notzel and D. Lenstra. "New role for nonlinear dynamics and chaos in integrated semiconductor laser technology", *Phys. Rev. Lett.* **98**, 044101 (2007)

[2] M. P. Vaughan, I. Henning, M. J. Adams, L. J. Rivers, P. Cannard and I. F. Lealman, "Mutual optical injection in coupled DBR laser pairs". *Optics Express* **17**, 2033-2041 (2009).

[3] D. Labukhin, C.A. Stolz, N. Zakhleniuk, R. Loudon and M. J. Adams, "Nonlinear dynamics of multi-section tunable lasers", *IEEE Journal of Quantum Electronics* **46**, 689-699 (2010).

[4] J. P. Toomey, D. M. Kane, S. Valling and A. M. Lindberg "Automated correlation dimension analysis of optically injected solid state lasers", *Optics Express*, **17**, 7592-7608 (2009)

[5] R. Todt and M.-C. Amann, "Influence of facet reflections on monolithic widely tunable laser diodes", *IEEE Photon. Technol. Lett.* **17**, 2520-2522 (2005)